Frog nest foams exhibit pharmaceutical foam-like properties

Brozio, Sarah; O'Shaughnessy, Erin M.; Woods, Stuart; Hall-Barrientos, Ivan; Martin, Patricia E.; Kennedy, Malcolm W.; Lamprou, Dimitrios A.; Hoskisson, Paul A.

1

2

Frog nest foams exhibit pharmaceutical foam-like properties

Sarah Brozio[1], Erin M. O'Shaughnessy[2], Stuart Woods[1], Ivan Hall-Barrientos[1], Patricia E. Martin[2], Malcolm W. Kennedy[3], Dimitrios A. Lamprou[4*] and Paul A. Hoskisson[1*]

[1] Strathclyde Institute of Pharmacy and Biomedical Sciences, University of Strathclyde, 161 Cathedral Street, Glasgow, G4 0RE, UK.

[2] Department of Biological and Biomedical Sciences, School of Health and Life Sciences, Glasgow Caledonian University, G4 OBA, UK.

[3] Institute of Biodiversity Animal Health & Comparative Medicine, Graham Kerr Building, University of Glasgow, Glasgow G12 8QQ, UK.

[4] School of Pharmacy, Queen's University Belfast, 97 Lisburn Road, Belfast BT9 7BL, UK

*Correspondence: d.lamprou@qub.ac.uk; Paul.hoskisson@strath.ac.uk, Tel.: +44 (0)141 548 2819.

17

18

19

Abstract

Foams have frequently been used as systems for the delivery of cosmetic and therapeutic molecules; however, there is high variability in the foamability and long-term stability of synthetic foams. The development of pharmaceutical foams that exhibit desirable foaming properties, delivering appropriate amounts of the active pharmaceutical ingredient (API) and that have excellent biocompatibility is of great interest. The production of stable foams is rare in the natural world; however, certain species of frogs have adopted foam production as a means of providing a protective environment for their eggs and larvae from a predators and parasites, to prevent desiccation, to control gaseous exchange, temperature extremes, and to reduce UV damage. These foams show great stability (up to 10 days in tropical environments) and are highly biocompatible due to the sensitive nature of amphibian skin. This work demonstrates for the first time, that nests of the Túngara frog (*Engystomops pustulosus*) is stable *ex situ* with useful physiochemical and biocompatible properties and is capable of encapsulating a range of compounds, including antibiotics. These protein foam mixtures share some properties with pharmaceutical foams and may find utility in a range of pharmaceutical applications such as a topical drug delivery systems (DDS).

Introduction

Foams have been used as delivery systems or vehicles to deliver cosmetic and therapeutic molecules to normal and injured skin since the 1970's[1–5]. Yet the long-term stability of liquid aqueous foams has been a challenge, with some formulations offering useful foamability properties (e.g. foam expansion time), but poor stability[6]. There has been some progress made through the combination of various foam and surfactant components to create high foamability and long-term foam stability[6–9]. However, the development of biocompatible, liquid foams with high foamability and long-term stability remains a challenge in materials science[6]. A range of foams is already in use for topical treatments, such as Ibuprofen foams (Biatain® Ib) used to relieve a wide range of exuding wounds, urea-containing foams (KerraFoam) to help alleviate the symptoms of psoriasis, and antibiotic foams containing clindamycin and other antimicrobials such as silver sulfacetamide[2,4]. A major advantage of medicated foams is their ability to cover large surface areas, while containing highly concentrated drugs for topical treatment[1]. One major difficulty can be the delivery of an adequate concentration of active pharmaceutical ingredients (APIs) for treatment over a sustained period, therefore often necessitating repeated, regular applications. In the case of open wounds and burns, regular removal of dressings may lead to increased infection risk and damage to healing surfaces, aid the emergence of antimicrobial resistance through the delivery of sub-minimum inhibitory concentrations of antibiotics, ultimately resulting in reduced infection control and wound healing[10]. Liposomes have proposed for dermatological applications; however, are exhibit major stability issues. There is therefore a need for the development of biomaterials that allow extended times between application combined with high stability and improved biocompatibility; natural foams can provide these benefits.

Anurans (frogs) exhibit enormous diversity in reproductive strategies and styles[11], and many species of tropical and subtropical frog lay their eggs in stable proteinaceous foams that differ in composition between species. Foam-nesting behaviour, thought to have evolved as a means to avoid aquatic predators, prevent desiccation of eggs, control gaseous exchange, buffer temperature extremes, reduce solar radiation damage, and protect eggs from microbial colonisation[12]. Stable biological foams and foam-producing surfactants are rare in nature, presumably due to the requirement for high-energy input for their generation, and the potential of surface-active components to negatively affect cell and membrane function[13,14]. Frog nest foams are remarkable for their strong surfactant activity combined with harmlessness to naked eggs and sperm. The leptodactylid frogs of the neotropics are one such anuran lineage that has

72 evolved stable foams as an offspring protection mechanism. The nests of the Túngara frog

73 (*Engystomops pustulosus*) are remarkable in structures that act as incubation chambers for

74 eggs[15] (**Supp. Fig. 1A & B;** https://doi.org/10.6084/m9.figshare.13281416.v1), allowing

75 rapid growth and development of embryos, offering a protective environment against predation,

76 whilst providing temperature regulation and oxygen transfer for optimal growth conditions.

77 These nests, there are not destroyed by microbes during larval development despite construction

78 within highly-microbe-rich water[16]. The foam nest structure is highly stable, remaining

79 assembled for as much as 10 days in the tropical environment[17,18], yet the surfactant activity

80 of the foam does not cause damage to the sperm, eggs or developing embryos[13]. The main

81 surfactant protein within these nests is an 11kDa protein, Ranaspumin-2 (RSN-2), which does

82 not disrupt biological membranes or cells, but it still provides sufficient surfactant activity at

83 the air-water interface to allow foam formation[19]. The RSN-2 protein appears to form a

84 clamshell-like structure, which can undergo an unfolding conformational change to expose

85 nonpolar patches on the protein surface to the air, while highly polar regions remain in contact

86 with the water interface to provide the surfactant activity. RSN-2 has been successfully used in

87 industry as a surfactant in nanoparticle production[20], but there could be great potential for the

88 whole nest foam protein composition to be used in a range of pharmaceutical applications.

89 Here we show that the unseparated, total protein mixture of *E. pustulosus* nest foam is stable *ex*

90 *situ* for extended periods with useful physiochemical and biocompatible properties and does

91 not the need of the addition of oxygen as with other drug delivery systems ([21]; DDS) and may

92 be used to encapsulate a range of hydrophobic and hydrophilic model compounds. These data

93 suggest that anuran-derived protein foams may have broad potential applications in

94 pharmaceutics and as DDSs.

95

Results & Discussion

Biophysical properties of Tungara frog foam preparation

The composition and properties of DDSs can determine the effectiveness of drug release, and while several factors may affect drug release, the thermodynamics driving the passive diffusion process is key[22]. Thus, increasing and stabilising the local concentration of the permeant is the simplest strategy to facilitate bioavailability[3]. The protein composition of *E. pustulosus* foam fluid was analysed by SDS-PAGE (**Supp. Fig. 1C;** https://doi.org/10.6084/m9.figshare.13281416.v1), confirming previous work that foam from this species contains six major proteins ranging between 10 and 40kDa in size[18] and that the foam nests used in this study were of typical composition. We observed no variation between collection years or from nests collected at different locations in Trinidad and all foam collected was checked by SDS-PAGE and were of the composition previously detailed in [17,18,19] and **Supp. Fig. 1C.** CD spectra of the samples showed a negative maximum at 215 nm and a positive maximum at 194 nm, (**Fig. 1A**) indicating that, cumulatively, the protein mixture in the foam fluid comprises predominately β-sheet structures. Further insight into secondary structure of the foam mixture was obtained by FTIR, which also exhibited spectra consistent with overall dominance of β-sheet structures (**Fig 1B**;[23]). For both foam solutions, transitions were observed at ~1680 cm^{-1}, which are frequencies characteristic of Amide I band, signifying C=O bond stretches typically engaged in β-sheet bonded network structures. These data support previous observations that average secondary structure content of the proteins is predominantly β-sheet[18] and indicates that the centrifugation steps in the preparation of the foam for these experiments does not alter the overall structure and composition of the foam from the wild *E. pustulosus* nests.

Fig. 1
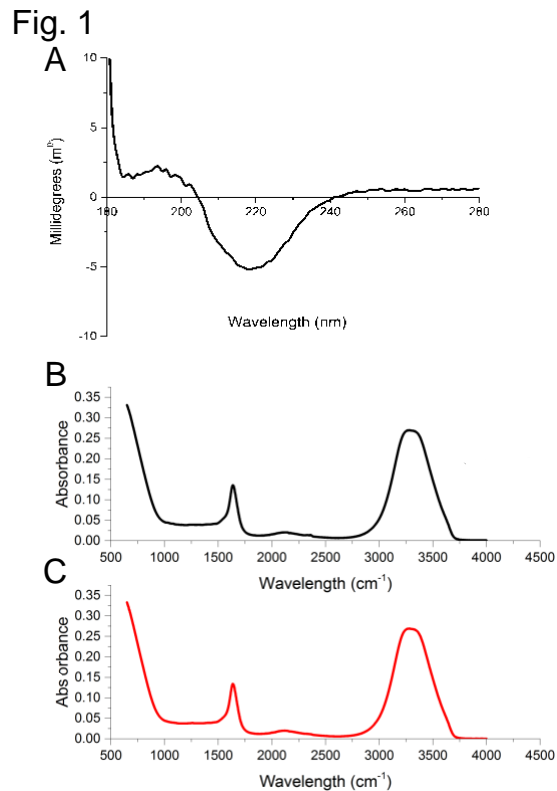
Figure. 1. Structural characterisation of *E. pustulosus* nest foam proteins. 1A: Circular Dichroism of foam fluid using 0.1mm pathlength cuvettes containing 1mg/ml protein foam fluid solution. **1B:** Fourier Transform Infrared Spectroscopy (FTIR) foam fluid **(B)** and whole foam **(C)**. For both CD and FTIR spectra were corrected for baseline and buffer effects each measurement was carried out in triplicate and the mean of the data is presented.

To investigate the viscoelastic properties of the foam, oscillation sweep experiments were employed by rheology. The whole foam fluid was found to tolerate up to 100 Pa of shear stress force before it reaches a breaking point, at which the elastic modulus of the foam decreases and foam structure and stability is lost (**Fig. 2A**). Time sweep experiments indicated that up to 1500 s the foam preparation moduli are unchanged by stress and frequency. After 1500 s both elastic and viscosity moduli increase demonstrating that water is being lost from the foam (**Fig. 2B**). It has been suggested that stress increases the chances of water loss from the foam followed by coarsening, which leads to an increase in viscoelasticity[24]. The *E. pustulosus* whole foam is able to withstand shear stress and pressure before breaking down, demonstrating the long-lasting stability that may be observed in nature. Pharmaceutical foams are typically required to remain stable in order to be properly manipulated while being applied, but have low shear allowing them to break down shortly thereafter[25,26]. The foam derived from *E. pustulosus*

6

has exhibits long-term stability in harsh tropical environments (e.g. heat, high level exposure to ultraviolet light, and physical disruption) and behaves differently from typical pharmaceutical foams[2]. The *E. pustulosus* foam is stable enough to be manipulated and able to withstand shear forces, suggesting potential for the delivery drugs over prolonged periods.

Fig. 2
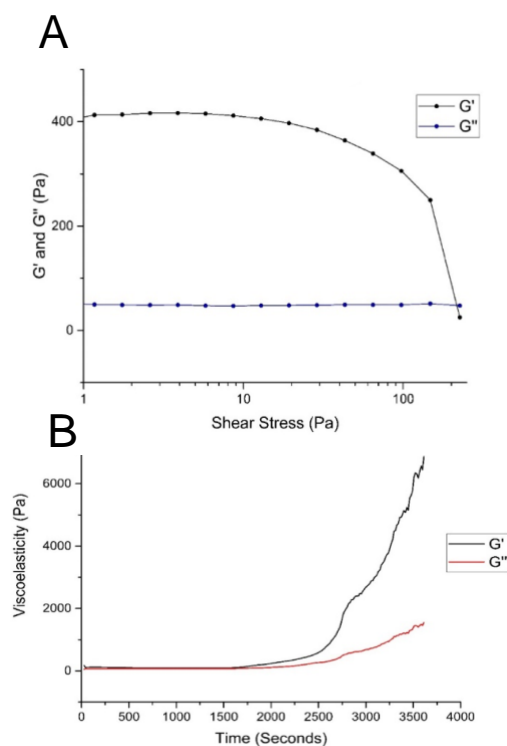
Figure 2. Viscoelastic properties of *E. pustulosus* nest foam. 2A: Time sweep rheology data for foam, showing both elastic (G') and viscous (G'') moduli. Stress was set at 100 Pa, and carried out over 1 hour. **2B:** Oscillation sweep rheology data for *E. pustulosus* foam, showing both elastic (G') and viscous (G'') moduli. Shear stress was increased from 1 Pa to 200 Pa. Each measurement was taken in triplicate at 20^0C.
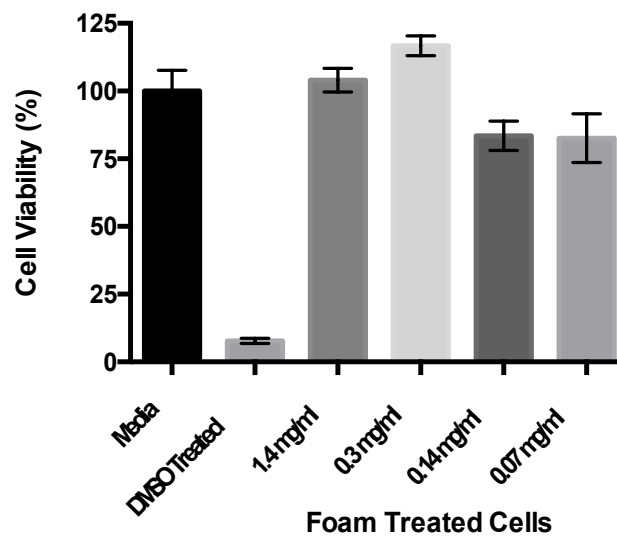
Frog foam biocompatibility with human epithelial cells

To investigate the susceptibility of mammalian cells to any possible toxic effects of the foam, cells were cultured in the presence of foam fluid and potential toxicity was assayed using an MTT-based cell viability assay. Exposing HaCaT keratinocyte cells to a range of *E. pustulosus* foam concentrations did not affect the overall cell viability and multiplication of the cells (**Fig. 3**). The higher foam fluid concentrations to which the cells were exposed are representative of foam concentration present in *E. pustulosus* nests (1-2mg/ml protein[17]). Cells exposed to the foam behave in the same manner as untreated control cells, demonstrating that the foam proteins from *E. pustulosus* are non-toxic to epithelial cells and are therefore unlikely to cause damage to the skin or underlaying tissues if used as a topical drug delivery system. The foam and its protein components are already known to be harmless to human erythrocytes [27]. This high degree of biocompatibility is consistent with the foam and its precursor components being harmless to naked amphibian sperm, eggs, and oviduct surfaces of the frogs[27].

Fig. 3

Fig. 3. Biocompatibility of *E. pustulosus* nest foam with human epithelial cells. MTT assay of HaCaT cell percentage viability following exposure to a range of fluid foam concentrations over 24 hours at 37^{0}C. Each treatment was performed in triplicate, and media alone was used as normal viability control (100%), and cells were treated with DMSO for non-viable control. Treatments were a dilution of fluid foam protein concentrations - 1.4 mg/ml, 0.3 mg/ml, 0.14 mg/ml and 0.07 mg/ml respectively. Error bars represent the standard deviation of the data.

In vitro release of drug-loaded frog foam

A single foam cell is defined as a bubble of gas enclosed in a liquid film that can be polyhedral or circular, heterogeneous or homogeneous, and usually range between 0.1 and 3mm in diameter[25]. The cell structure of *E. pustulosus* nest-foam was evaluated microscopically and the foam cell sizes measured (**Fig. 4A**). The foam cells in all samples were found to be a heterogeneous mixture of uneven, spherical and polyhedral cells with a Feret diameter ranging from 10-800 μm, falling in the normal range of foam cell size of foams that have been used previously in pharmaceutical applications[25].

The relative density of the foam was found to be 0.25 g of protein/ml. AFM PeakForce analysis of the fluid foam and gel foam indicated consistency of the individual adhesion force (F_{ad}) measurements in each foam forms (**Fig. 4B**) indicating that the foam surface forces are homogeneous across the surface of each form. Moreover, in the case of the fluid foam, the F_{ad} is higher and the AFM images shows the formation of ~200 nm droplets as the foam was dried on to mica surfaces. This combination of low density and high structural stability is unusual and suggests anuran foam-nest proteins exhibit similar properties to pharmaceutical foams.

Fig. 4

A

B

Fluid foam   Solid foam

Fig. 4. Drug loading of *E. pustulosus* nest foam does not alter the structure of the foam.
4A. Foam cell diameter measurements scatter plot. Feret diameter of each foam cell/bubble was measured using Fiji software. Bars on the scatter encompass 10-90% of the data points, with the central horizontal line representing mean values. Above the scatter graph are representative images of unloaded foam, foam loaded with 1 mg/ml NR and foam loaded with 1mg/ml calcein. All images were taken using freshly defrosted foam. **4B.** Atomic Force Microscopy PeakForce analysis of foam fluid and gel foam to investigate the consistency of the adhesion force (F_{ad}) in the foam.

To evaluate the drug release behaviour of *E. pustulosus* foam, experiments were performed using a dialysis-based method where two model compounds (one hydrophobic and one hydrophilic), NR and calcein, were encapsulated in the foams. Calcein exhibits a "burst-type" release profile from the foam, whereas NR is discharged at a linear rate over seven days (168 hours; **Fig. 5A & B**). These data indicate that the whole foam can absorb and release both hydrophobic (NR) and hydrophilic (calcein) molecules and release these at different rates over a prolonged period, with up to 85% of the loaded dye released up to seven days (168 hours). Longer time periods were not studies as typically release of APIs from foams occurs on minute to hour timescales [2], however seven days is approaching the lifetime of the foam in the natural environment [15]. Moreover, the loading of the nest foam with NR or calcein did not alter the cell size or shape of the foam (**Fig.** 4). The unique release properties associated with the *E. pustulosus* foam may in part be explained by the unique surfactant properties and 'clam shell' structure adopted by at least one member of the protein complex in solution. RSN-2 is an amphiphilic polypeptide which exhibits no obvious hydrophobic patches or structural features that are normally associated with surfactant proteins [14]. RSN-2 is able to adopt an open 'clam-shell' configuration to present the hydrophobic faces of the protein to the interface whilst maintaining contact of the polar regions of the protein with the aqueous phase. This may enable the *E. pustulosus* foam proteins modify their structure according to the nature of the drug molecule that is loaded, resulting in the different release profiles for hydrophobic or hydrophilic drug mimics we observed. This property is likely to broaden their potential application as a DDS allowing *E. pustulosus* foam to be loaded with a range of APIs.

To test the ability of the foam to release a clinically relevant drug molecule, the whole foam loaded in the same manner as for the previous two molecules with the red-pigmented, polyketide antibiotic rifampicin. Polyketide antibiotics have successfully been delivered using foam DDSs, thus rifampicin offers a potentially useful comparison to existing systems [2] and is amenable to spectroscopic analysis. The dialysis method of release showed that rifampicin was released at a steady rate over the first five hours with a release of around 80% of loaded antibiotic, followed by a second, slower phase of release (**Fig. 5C**).

To further investigate the release of drug molecules from *E. pustulosus* foam, a novel trans-well-based release assay was developed, which emulates delivery of the foam preparation across a more complex protein coated surface. Foam was loaded in to a collagen-coated transwell sat in a 24-well tissue culture plate containing 1 ml of PBS and release of drug molecule was determined through the assay of the amount of rifampicin that passed from the

foam through the transwell membrane. In the transwell assay, around 50% of rifampicin was
also released over a 48 hrs (**Fig. 5D**).
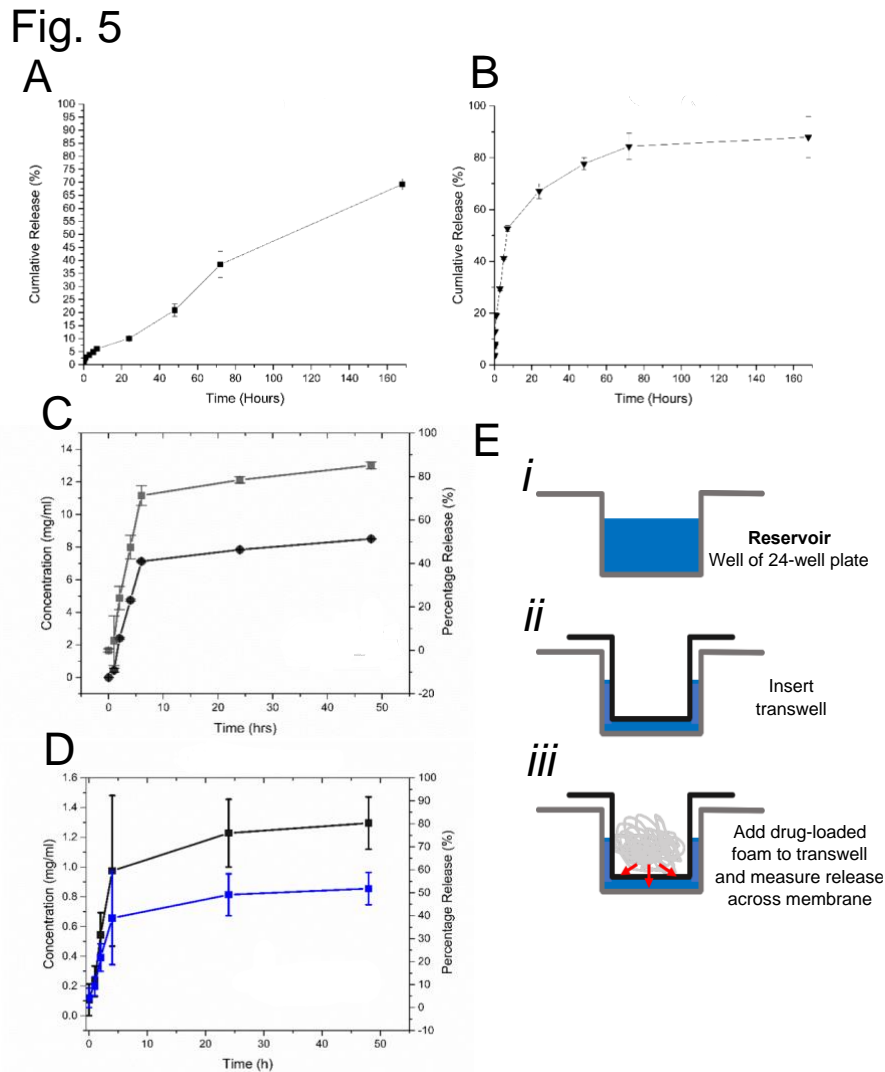
Fig. 5

Fig. 5. *E. pustulosus* nest foam can take up and release model compounds and drug molecules. 5A:
Cumulative release of the dye NR from loaded whole foam over 168 hrs using the dialysis method.
5B: Cumulative release of the dye calcien from loaded whole foam over 168 hrs using the dialysis
method. **5C:** Cumulative release of the antibiotic rifampicin from loaded whole foam over 168 hrs
using the dialysis method; -●- concentration (mg/ml); -■- percentage release of the dye or drug. **5D:**
Release of rifampicin using novel transwell method; -■- concentration (mg/ml of protein); -■-
percentage release of rifampicin. Each point represents the mean of data collected in triplicate and
error bars indicate the standard deviation of the data. Sink conditions satisfied by replacing sample
volume with fresh buffer at each sample point. Dye release concentrations were calculated using
spectrophotometric standard curves for respective dye or drug. **5E:** Schematic representing the
experimental set-up using the novel transwell release assay, with reservoirs of 24-well plate filled

with buffer (*i*), the insertion of the permeable transwell (*ii*), and the addition of drug-loaded foam to the transwell to allow drug release across the transwell membrane which can be quantified in the reservoir.

This novel transwell assay for investigating compound release from foams offers a simpler route to assaying drug release from foams and other aqueous-based materials that does not require the manipulation of dialysis tubing. Moreover, the release mimics clinical applications through release from a single face of the transwell (A schematic of the Transwell-based assay is provided in **Fig. 5E**) with the advantage that transwells are available in a number of sizes and pore diameters to suit a range of needs.

These data indicate that the frog foam can be loaded with drug molecules and has an extended release profile when compared to existing pharmaceutical foams, with release over days rather than minutes or hours [28]. The foam from *E. pustulosus* is stable and the API release is relatively slow with the foam potentially acting as a barrier in the local environment. The *E. pustulosus* foam also compares well with release of rifampicin from nanoparticles loaded with antibiotics of the same chemical class, where 80-90% of release occurs, but within an 8 h time window[29].

Many nanoparticle-based systems release their drug-load rapidly resulting in ineffective long-term treatment possibilities[30] and have exhibited some toxic properties[31]. The anuran foam-based preparations extend this release period to around 48 hrs depending on the nature of the compounds used, expanding the possible applications of frog foams. While there has been multiple antibiotic loaded liposomes[32–34](AmBisome, Lambin, Doxil) brought to market, little have transferred the applicability to topical conditions, and their efficiency is still lacking. Further, tetracycline (a polyketide antibiotic) loaded nanocomposite hydrogels that have been used for extended release delivery through the skin, released of maximum of 15% of their antibiotic load [33]. Foams are considered more popular with patients than gels[2], and a stable foam may provide a solution to both these issues. Previous studies of pharmaceutical foams have investigated the immediate delivery of drugs through to the dermis by exploiting the fast breakdown of foam preparations, but rarely have they been used for long-term drug release[2]. The foam derived from *E. pustulosus* provides a material with potential due to its intermediate release properties, where API uptake is efficient, it has high stability and the slow release properties enable continuous release over a clinically useful period of time.

Conclusions

There is an increased interest in drug delivery systems to refine the use of antimicrobial drugs currently available on the market, which may enable novel delivery systems help combat the rise of antimicrobial resistance in the clinic. Anuran foams from reproductive nests may provide a novel area for future investigation in controlled release. Anuran foam nests share properties with pharmaceutical foams, they are highly biocompatible, durable and stable, and have excellent drug release properties. They exhibit few of the issues associated with fabric-based drug release such as instability, rapid release characteristics or toxicity. These advantages suggest that with further research anuran foams have potential for use as a pharmaceutical foam.. To fully meet the demands of modern pharmaceutical manufacture, formulation, sterility, product consistency and for reasons of sustainability, it is envisaged that heterologous production of these proteins will be required for their future exploitation in the clinic. It has been shown that at least one protein is amenable to production in bacterial protein production systems [19]. Further research is required to understand the interaction and properties of the six major foam proteins in combination and there may be potential to modify the protein mixture using heterologous expression, for example, simplify the composition of the foam mixture, modify stability with different combinations of component proteins etc. There is also potential for the use of individual proteins from the nest protein complex as pharmaceutical ingredients given their surfactant properties. It is known that at least one member of the *E. pustulosus* foam complex (RSN-2) can be whipped to form short-lived (lasting hours rather than days before collapsing) foams that superficially appear similar to natural foam nests [14]. These frog foam nest proteins offer a number of avenues for exploitation in the future, but will require further research to fully exploit their potential.

Materials and Methods

Materials

Nile red (NR), calcein, ethanol 97% (v/v), phosphate buffered saline (PBS) tablets (pH 7.2) were all purchased from Sigma and MTT (3-(4,5-dimethylthiazol-2-yl)-2,5-diphenyltetrazolium was purchased from Thermofisher.

Collection of *Engystomops pustulosus* foam

Freshly laid foam nests or adult frogs in amplexus (allowed to lay in captivity, before release) were collected from a number of sites in northern Trinidad in June and July of 2014, 2015 and 2016. Nests were removed from the surface of the water in which they were produced (An *in situ* nest can be seen in **Supp. Fig. 1B**) and the eggs were removed manually before being stored at -20^0C for transfer to the Glasgow, where they were stored at -80^0C. Nest foam was pooled and checked by SDS-PAGE to ensure the protein integrity (**Supp. Fig. 1C**). Foam was freshly defrosted for all experiments with no further processing being required as foam maintains its integrity upon freeze/thawing. Soluble foam material ('foam fluid') was produced by centrifuging whole foam for 10 min (16,000 x *g*), providing a solution with approximately ~2 mg/ml protein. This also yields a supernatant/pellicle residual of semi-solid compressed foam ('gel foam') on top of the foam fluid layer.

Microscopy

Optical microscopy: Whole foam was defrosted at room temperature before use. All foam images were taken using transmitted light on a Nikon SMZ1500 stereomicroscope with images acquired using a DFK 33UX264 CMOS camera (The Imaging Source Europe GmbH, Germany) using NIS-Elements AR.3.2 software. Fiji software (https://fiji.sc/) from the ImageJ (https://imagej.net) package was used for image analysis.

Atomic force microscopy (AFM): Samples (5 μl) of foam were deposited onto a freshly cleaved mica surface (1.5 cm x 1.5 cm; G250-2 Mica sheets 25 mm x 25 mm x 0.15 mm; Agar Scientific Ltd, Essex, UK) and left to dry at room temperature for 1h before imaging. The images were obtained by scanning the mica surface in air under ambient conditions using a Scanning Probe Microscope (MultiMode® 8, Digital Instruments, Santa Barbara, CA, USA; Bruker Nanoscope analysis software Version 1.40), operating using the PeakForce QNM mode. The AFM measurements were obtained using ScanAsyst-air probes, for which the spring constant (0.58

349 N/m; Nominal 0.4 N/m) and deflection sensitivity had been calibrated, but not the tip radius
350 (the nominal value used was 2 nm).

Sodium Dodecyl Sulfate Poly-Acrylamide Gel Electrophoresis (SDS-PAGE)

352 Solid and liquid foam samples were electrophoresed on precast NuPAGE 15% polyacrylamide
353 Bis-Tris gels (Invitrogen) at 120V using 4 X SDS reducing loading buffer (Invitrogen). Each
354 gel was stained with InstaBlue Coomassie protein stain for ~45 min.

Circular Dichroism Spectroscopy (CD)

356 CD was used to investigate the overall secondary structure content of the proteins. Spectra were
357 acquired using a Chirascan Plus (Applied Photophysics) instrument using a 0.1mm quartz
358 cuvette (Hellma) at 20^0C. All samples (10 mg/ml protein) were measured in the far-UV in a
359 wavelength range of 180 nm to 280 nm range, with step size of 1 nm, bandwidth of 1 nm, and
360 reading time of 1 s per nm. Triplicate measurements were taken for each sample run, baseline
361 peak, PBS control and foam sample spectra, with triplicate spectra then averaged. Baseline and
362 PBS traces where subtracted from the sample spectra before secondary structure predictions
363 were made. All data analysis was performed using Global3 software and Excel.

Fourier transform infrared spectroscopy

365 Fourier transform infrared (FTIR) spectroscopy was carried out using a Nicolet iS10 Smart iTR
366 spectrophotometer (Thermo Scientific). Solid and liquid foam spectra were recorded in the
367 range on 4000 cm^{-1} and 500 cm^{-1}, over 128 scans at a resolution of 4 cm^{-1} and an interval of 1
368 cm^{-1}. Background spectra were measured and the foam spectra were corrected accordingly.

Rheology

370 Rheology measurements were determined using a HAAKE MARS Rotational Rheometer
371 (Thermo Scientific). Foam samples were subjected to oscillation sweeps and time sweeps. All
372 experiments were carried out using P20 upper plate and TM20 lower plate. The oscillation
373 sweeps were completed with a 1 mm gap and 0.1 Pa to 200 Pa range. Time sweep experiments
374 were run for 1 h, at 100 Pa and 3 Hz using a 0.5 mm gap. Data points were collected in triplicate
375 and averaged before analysis was carried out.

MTT cell viability assay

377 HaCaT cells (CLS, Eppelheim, Germany), a model human keratinocyte cell line were cultured
378 in Dulbecco's modified Eagle's medium (DMEM) containing 4.5 g/l glucose supplemented

with 10% (v/v) fetal bovine serum, 2 mM L-glutamine and 50 units/ml penicillin/streptomycin (cDMEM; Lonza, Slough, UK). Soluble foam proteins were prepared as above, with the supernatant being passed the a 0.22 μm filter (Millex 33 mm) and subsequently concentrated using an Amicon 10 kDa spin filter. The protein concentration was determined by Bradford assay (BioRad). The HaCaT cells were plated onto 96 well plates ($\sim$1x10^3 cells per well and grown to 80% confluence) and were treated with buffer containing foam proteins (concentrations indicated in the figures) prior to incubation at 37 ^{0}C for 24 hours. After 24 hours the media was removed from the cells, and replaced with 50 μl of fresh media and 50 μl of MTT (5mg/ml) and incubated for 1 h at 37 ^{0}C. This was followed by replacing the media with 100 μl DMSO and further incubation in the dark at room temperature for 30 minutes prior to reading the absorbance at 570nm[35]. Results were expressed as the % cell viability compared to non-treated cells ± SD of the data.

In vitro release of model compounds

Aliquots (500 mg) of whole foam were loaded with dye by mixing with either 400 μl of Nile Red (NR; hydrophobic; 1 mg/ml in ethanol) or calcein (hydrophilic; 1 mg/ml in ethanol). All free liquid containing NR or calcein was encapsulated within the foam following mixing. The mixture was the placed in dialysis tubing and sealed before being submerged in 10 ml PBS at 37 ^{0}C (pH 7; for NR-based release experiments, a 1:1 mixture of ethanol and PBS was used). The release experiments were carried out at 37 ^{0}C, over 168 hours. To satisfy the perfect-sink conditions, which allow for the determination of the diffusion parameters, the supernatant was replaced with fresh PBS at 37 °C at each time point (indicated in the graphs). The concentration of model compound in each sample was determined spectrophotometrically at 490 nm (calcein) or 590 nm (NR) and the concentration determined with reference to standard control calibration curves. Experiments were performed in triplicate.

In vitro Antibiotic release

Two *in vitro* techniques were used to investigate the release of the antibiotic rifampicin.

Dialysis: Aliquots (400 mg) of foam were mixed with 400 μl of rifampicin (25 mg/ml) as above. The loaded foam was placed into dialysis tubing, sealed and submerged in 10 ml of PBS. This was incubated at 37 ^{0}C for 48 hours. Samples (1 ml) were taken and fresh media added to maintain sink conditions. Samples where measured by spectrophotometrically at 475 nm[36] against a calibration curve.

410 *Transswell:* Aliquots of foam (100 mg) were mixed with 100 µl of rifampicin (25mg/ml).

411 Rifampicin loaded foam was the placed into a transwell collagen-coated permeable support (0.4

412 µm; Nunc). Each support was inserted into 24 well plate well containing 600ul of PBS. The

413 plate was then incubated for 48 hours at 37 ^{0}C. PBS (600µl) was collected from a well for each

414 time point, and the absorbance measured at 475nm, in triplicate.

415

Supporting Information.

Acknowledgements

Conflict of interest

All authors declare that they have no conflict of interest in relation to this work.

References

1. Haznar-Garbacz D, Garbacz G, Weitschies W. 2019 Development of oral foams for topical treatment of inflammatory bowel disease. *J Drug Deliv Sci Tec* **50**, 287–292. (doi:10.1016/j.jddst.2019.01.022)

2. Zhao Y, Jones SA, Brown MB. 2010 Dynamic foams in topical drug delivery. *J Pharm Pharmacol* **62**, 678–84. (doi:10.1211/jpp.62.06.0003)

3. Gennari CGM, Selmin F, Minghetti P, Cilurzo F. 2019 Medicated foams and film forming dosage forms as tools to improve the thermodynamic activity of drugs to be administered through the skin. *Curr Drug Deliv* **16**, 461–471. (doi:10.2174/1567201816666190118124439)

4. Zhao Y, Brown MB, Jones SA. 2010 Pharmaceutical foams: are they the answer to the dilemma of topical nanoparticles? *Nanomed Nanotechnol Biology Medicine* **6**, 227–236. (doi:10.1016/j.nano.2009.08.002)

5. Svagan AJ, Benjamins J-W, Al-Ansari Z, Shalom DB, Müllertz A, Wågberg L, Löbmann K. 2016 Solid cellulose nanofiber based foams - Towards facile design of sustained drug delivery systems. *J Control Release Official J Control Release Soc* **244**, 74–82. (doi:10.1016/j.jconrel.2016.11.009)

6. Russo M, Amara Z, Fenneteau J, Chaumont-Olive P, Maimouni I, Tabeling P, Cossy J. 2020 Stable liquid foams from a new polyfluorinated surfactant. *Chem Commun* (doi:10.1039/d0cc02182b)

7. Fameau A-L *et al.* 2011 Smart Foams: Switching Reversibly between Ultrastable and Unstable Foams. *Angewandte Chemie Int Ed* **50**, 8264–8269. (doi:10.1002/anie.201102115)

8. Arriaga LR, Drenckhan W, Salonen A, Rodrigues JA, Íñiguez-Palomares R, Rio E, Langevin D. 2012 On the long-term stability of foams stabilised by mixtures of nano-particles and oppositely charged short chain surfactants. *Soft Matter* **8**, 11085. (doi:10.1039/c2sm26461g)

9. Stocco A, Carriere D, Cottat M, Langevin D. 2010 Interfacial Behavior of Catanionic Surfactants. *Langmuir* **26**, 10663–10669. (doi:10.1021/la100954v)

461   10. Heunis TDJ, Dicks LMT. 2010 Nanofibers offer alternative ways to the treatment of skin
462   infections. *J Biomed Biotechnology* **2010**, 510682. (doi:10.1155/2010/510682)

463   11. Crump ML. 2015 Anuran Reproductive Modes: Evolving Perspectives. *J Herpetol* **49**, 1–
464   16. (doi:10.1670/14-097)

465   12. Pereira EB, Pinto-Ledezma JN, Freitas CG de, Villalobos F, Collevatti RG, Maciel NM.
466   2017 Evolution of the anuran foam nest: trait conservatism and lineage diversification. *Biol J*
467   *Linn Soc* **122**, 814–823. (doi:10.1093/biolinnean/blx110)

468   13. Cooper A, Kennedy MW. 2010 Biofoams and natural protein surfactants. *Biophys Chem*
469   **151**, 96–104. (doi:10.1016/j.bpc.2010.06.006)

470   14. Cooper A, Vance SJ, Smith BO, Kennedy MW. 2017 Frog foams and natural protein
471   surfactants. *Colloids   Surfaces   Physicochem   Eng   Aspects* **534**,   120–129.
472   (doi:10.1016/j.colsurfa.2017.01.049)

473   15. Downie, R J. 1988 Functions of the foam in the foam-nesting leptodactylid *Physalaemus*
474   *pustulosus*. *The Herpetological Journal* **1**, 302–307.

475   16. Downie, R. J. 1990 Functions of the foam in foam-nesting leptodactylids anti-predator
476   effects of Physalaemus pustulosus foam. **1**, 501–503.

477   17. Fleming RI, Mackenzie CD, Cooper A, Kennedy MW. 2009 Foam nest components of the
478   túngara frog: a cocktail of proteins conferring physical and biological resilience. *Proceedings*
479   *of the Royal Society B: Biological Sciences* **276**. (doi:10.1098/rspb.2008.1939)

480   18. Cooper A, Kennedy MW, Fleming RI, Wilson EH, Videler H, Wokosin DL, Su T, Green
481   RJ, Lu JR. 2005 Adsorption of Frog Foam Nest Proteins at the Air-Water Interface. *Biophys J*
482   **88**, 2114–2125. (doi:10.1529/biophysj.104.046268)

483   19. Mackenzie CD, Smith BO, Meister A, Blume A, Zhao X, Lu JR, Kennedy MW, Cooper A.
484   2009 Ranaspumin-2: Structure and Function of a Surfactant Protein from the Foam Nests of a
485   Tropical Frog. *Biophysical Journal* **96**. (doi:10.1016/j.bpj.2009.03.044)

486   20. Choi H-J, Ebersbacher CF, Myung NV, Montemagno CD. 2012 Synthesis of nanoparticles
487   with frog foam nest proteins. *J Nanopart Res* **14**, 1092. (doi:10.1007/s11051-012-1092-1)

488 21. Suvarnapathaki S, Wu X, Lantigua D, Nguyen MA, Camci-Unal G. 2019 Breathing life
489 into engineered tissues using oxygen-releasing biomaterials. *Npg Asia Mater* **11**, 65.
490 (doi:10.1038/s41427-019-0166-2)

491 22. Freire MCLC, Jr. FA, Marcelino HR, Picciani PH de S, Silva KG de H e, Genre J, Oliveira
492 AG de, Egito EST do. 2017 Understanding Drug Release Data through Thermodynamic
493 Analysis. *Materials* **10**, 651. (doi:10.3390/ma10060651)

494 23. Kong J, Yu S. 2007 Fourier Transform Infrared Spectroscopic Analysis of Protein
495 Secondary Structures. *Acta Bioch Bioph Sin* **39**, 549–559. (doi:10.1111/j.1745-
496 7270.2007.00320.x)

497 24. Marze SPL, Saint-Jalmes A, Langevin D. 2005 Protein and surfactant foams: linear
498 rheology and dilatancy effect. *Colloids Surfaces Physicochem Eng Aspects* **263**, 121–128.
499 (doi:10.1016/j.colsurfa.2005.01.014)

500 25. Arzhavitina A, Steckel H. 2010 Foams for pharmaceutical and cosmetic application. *Int J*
501 *Pharmaceut* **394**, 1–17. (doi:10.1016/j.ijpharm.2010.04.028)

502 26. Kealy T, Abram A, Hunt B, Buchta R. 2007 The rheological properties of pharmaceutical
503 foam: implications for use. *Int J Pharmaceut* **355**, 67–80. (doi:10.1016/j.ijpharm.2007.11.057)

504 27. Clarke BT. 2007 The natural history of Amphibian skin secretions, their normal functioning
505 and potential medical applications. *Biol Rev* **72**, 365–379. (doi:10.1111/j.1469-
506 185x.1997.tb00018.x)

507 28. Parsa M, Trybala A, Malik D, Starov V. 2019 Foam in pharmaceutical and medical
508 applications. *Curr Opin Colloid In* **44**, 153–167. (doi:10.1016/j.cocis.2019.10.007)

509 29. Sung JC, Padilla DJ, Garcia-Contreras L, Verberkmoes JL, Durbin D, Peloquin CA, Elbert
510 KJ, Hickey AJ, Edwards DA. 2009 Formulation and pharmacokinetics of self-assembled
511 rifampicin nanoparticle systems for pulmonary delivery. *Pharmaceut Res* **26**, 1847–55.
512 (doi:10.1007/s11095-009-9894-2)

513 30. Sabaeifard P, Abdi-Ali A, Soudi MR, Gamazo C, Irache JM. 2016 Amikacin loaded PLGA
514 nanoparticles against *Pseudomonas aeruginosa*. *European J Pharm Sci Official J European*
515 *Fed Pharm Sci* **93**, 392–8. (doi:10.1016/j.ejps.2016.08.049)

516 31. Toppo FA, Pawar RS. 2015 Novel drug delivery strategies and approaches for wound
517 healing. **2**, 12-20.

518 32. Azanza JR, Sádada B, Reis J. 2015 Liposomal formulations of amphotericin B: differences
519 according to the scientific evidence. *Revista Española De Quimioterapia Publicación Oficial*
520 *De La Sociedad Española De Quimioterapia* **28**, 275–81.

521 33. Namazi H, Rakhshaei R, Hamishehkar H, Kafil HS. 2016 Antibiotic loaded
522 carboxymethylcellulose/MCM-41 nanocomposite hydrogel films as potential wound dressing.
523 *Int J Biol Macromol* **85**, 327–334. (doi:10.1016/j.ijbiomac.2015.12.076)

524 34. Lee M-K. 2019 Clinical usefulness of liposomal formulations in cancer therapy: lessons
525 from the experiences of doxorubicin. *J Pharm Investigation* **49**, 203–214. (doi:10.1007/s40005-
526 018-0398-0)

527 35. Niles AL, Moravec RA, Worzella TJ, Evans NJ, Riss TL. 2013 High-Throughput Screening
528 Methods in Toxicity Testing. , 107–127. (doi:10.1002/9781118538203.ch5)

529 36. Benetton SA, Kedor-Hackmann ERM, Santoro MIRM, Borges VM. 1998 Visible
530 spectrophotometric and first-derivative UV spectrophotometric determination of rifampicin and
531 isoniazid in pharmaceutical preparations. *Talanta* **47**, 639–643. (doi:10.1016/s0039-
532 9140(98)00111-8)

533

534

Figure legends

Fig. 1. Structural characterisation of *E, pustulosus* nest foam proteins. 1A: Circular Dichroism of foam fluid using 0.1mm pathlength cuvettes containing 1mg/ml protein foam fluid solution. **1B:** Fourier Transform Infrared Spectroscopy (FTIR) foam fluid **(B)** and whole foam **(C)**. For both CD and FTIR spectra were corrected for baseline and buffer effects each measurement was carried out in triplicate and the mean of the data is presented.

Fig. 2. Viscoelastic properties of *E. pustulosus* nest foam. 2A: Time sweep rheology data for foam, showing both elastic (G') and viscous (G'') moduli. Stress was set at 100 Pa, and carried out over 1 hour. **2B:** Oscillation sweep rheology data for *E. pustulosus* foam, showing both elastic (G') and viscous (G'') moduli. Shear stress was increased from 1 Pa to 200 Pa. Each measurement was taken in triplicate at 20^0C.

Fig. 3. Biocompatibility of *E. pustulosus* nest foam with human epithelial cells. MTT assay of HaCaT cell percentage viability following exposure to a range of fluid foam concentrations over 24 hours at 37^0C. Each treatment was performed in triplicate, and media alone was used as normal viability control (100%), and cells were treated with DMSO for non-viable control. Treatments were a dilution of fluid foam protein concentrations - 1.4 mg/ml, 0.3 mg/ml, 0.14 mg/ml and 0.07 mg/ml respectively. Error bars represent the standard deviation of the data.

Fig. 4. Drug loading of *E. pustulosus* nest foam does not alter the structure of the foam. **4A**. Foam cell diameter measurements scatter plot. Feret diameter of each foam cell/bubble was measured using Fiji software. Bars on the scatter encompass 10-90% of the data points, with the central horizontal line representing mean values. Above the scatter graph are representative images of unloaded foam, foam loaded with 1 mg/ml NR and foam loaded with 1mg/ml calcein. All images were taken using freshly defrosted foam. **4B.** Atomic Force Microscopy PeakForce analysis of foam fluid and gel foam to investigate the consistency of the adhesion force (F_{ad}) in the foam.

Fig. 5. *E. pustulosus* nest foam can take up and release model compounds and drug molecules. 5A: Cumulative release of the dye NR from loaded whole foam over 168 hrs using the dialysis method. **5B:** Cumulative release of the dye calcien from loaded whole foam over 168 hrs using the dialysis method. **5C:** Cumulative release of the antibiotic rifampicin from loaded whole foam over 168 hrs using the dialysis method; -●- concentration (mg/ml); -■- percentage release of the dye or drug. **5D:** Release of rifampicin using novel transwell method;

567 -■- concentration (mg/ml of protein); -■- percentage release of rifampicin. Each point
568 represents the mean of data collected in triplicate and error bars indicate the standard deviation
569 of the data. Sink conditions satisfied by replacing sample volume with fresh buffer at each
570 sample point. Dye release concentrations were calculated using spectrophotometric standard
571 curves for respective dye or drug. **5E:** Schematic representing the experimental set-up using
572 the novel transwell release assay, with reservoirs of 24-well plate filled with buffer (***i***), the
573 insertion of the permeable transwell (***ii***), and the addition of drug-loaded foam to the transwell
574 to allow drug release across the transwell membrane which can be quantified in the reservoir.

575 **Supplementary Figure**

576 **Supplementary Fig. 1A.** Adult Túngara frog (*Engystomops pustulosus*). **B.** *In situ E.*
577 *pustulosus* foam nest. **C.** SDS-PAGE gel of *E. pustulosus* whole foam from a wild-collected
578 nest electrophoresed through a 4-20% Tris-Glycine NuPAGE gel under reducing conditions.
579 Proteins in the 10-30 kDa range are the ranaspumins (RSN described by Fleming et al., 2009 -
580 highlighted by red boxes. RSN molecular mass based on amino acid sequence: RSN-1, 14kDa;
581 RSN-2, 11kDa; RSN-3, 18kDa; RSN-4, 21kDa; RSN-5, 18kDa; RSN-6, 27kDa) **Marker:** 10-
582 200kDa Broad Range marker (New England Biolabs; #P7704).

583

584 **Reference**

585 Fleming, R. I., C.D. Mackenzie, A. Cooper, M.W. Kennedy, Foam nest components of the
586 Túngara frog: a cocktail of proteins conferring physical and biological resilience, Proceedings
587 of the Royal Society B: Biological Sciences. 276 (2009). doi:10.1098/rspb.2008.1939.

588

589